

High-Resolution, High-Pressure NMR Studies of Proteins

J. Jonas,* L. Ballard,# and D. Nash#

*Beckman Institute for Advanced Science and Technology, and #Department of Chemistry, School of Chemical Sciences, University of Illinois, Urbana, Illinois 61801 USA

ABSTRACT Advanced high-resolution NMR spectroscopy, including two-dimensional NMR techniques, combined with high pressure capability, represents a powerful new tool in the study of proteins. This contribution is organized in the following way. First, the specialized instrumentation needed for high-pressure NMR experiments is discussed, with specific emphasis on the design features and performance characteristics of a high-sensitivity, high-resolution, variable-temperature NMR probe operating at 500 MHz and at pressures of up to 500 MPa. An overview of several recent studies using 1D and 2D high-resolution, high-pressure NMR spectroscopy to investigate the pressure-induced reversible unfolding and pressure-assisted cold denaturation of lysozyme, ribonuclease A, and ubiquitin is presented. Specifically, the relationship between the residual secondary structure of pressure-assisted, cold-denatured states and the structure of early folding intermediates is discussed.

INTRODUCTION

Since Anfinsen and colleagues (Anfinsen, 1973) first studied the renaturation of reduced and unfolded ribonuclease A (RNase A), much effort has been expended in attempting to understand the relationships between the amino acid sequence, the structure, and dynamic properties of the native conformation of proteins. Recently, increasing attention has been focused on denatured and partially folded states, because determination of their structure and stability may provide critical insights into the mechanisms of protein folding (Kim and Baldwin, 1990; Creighton, 1993; Buck et al., 1994). The native conformations of hundreds of proteins are known in great detail from structural determinations by x-ray crystallography and, more recently, NMR spectroscopy. However, detailed knowledge of the conformations of denatured and partially folded states is lacking, which is a serious shortcoming in current studies of protein stability and protein folding pathways (Robertson and Baldwin, 1991).

Most studies dealing with protein denaturation have been carried out at atmospheric pressure with various physico-chemical perturbations, such as temperature, pH, or denaturants, as experimental variables. Compared to varying temperature, which produces simultaneous changes in both volume and thermal energy, the use of pressure to study protein solutions perturbs the environment of the protein in a continuous, controlled way by changing only intermolecular distances (Weber and Drickamer, 1983). In addition, by taking advantage of the phase behavior of water (Jonas, 1982), shown in Fig. 1, high pressure can substantially lower the freezing point of an aqueous protein solution. Therefore, by applying high pressure, one can investigate in

detail not only pressure-denatured proteins, but also cold-denatured proteins in aqueous solution.

The great potential of the high-resolution, high-pressure NMR techniques for studies of proteins (Jonas and Jonas, 1994) provided the motivation for our efforts in improving the performance of high-resolution, high-pressure NMR probes. We have discussed our own progress (Ballard et al., 1996) in the development of high-pressure NMR instrumentation, based on the autoclave-style approach, in which both the sample and the RF coil are located in a nonmagnetic, high-pressure vessel. In this contribution we focus on the very recent development (Ballard et al., 1998) of a high-sensitivity, high-resolution NMR probe operating at 500 MHz and at pressures of up to 500 MPa. Such probes are currently being used to obtain conventional 2D NMR spectra (e.g., COSY and NOESY spectra) of proteins on a routine basis.

One major application of NMR to protein chemistry is the use of hydrogen exchange kinetics as a probe of protein structure. Our group has recently applied this method to investigate structure in proteins denatured by high pressure at various temperatures. Previous work (Zhang et al., 1995; Konno et al., 1995; Wong et al., 1996) on pressure and cold denaturation has suggested that these methods can leave appreciable residual structure in proteins, particularly when compared to other methods such as thermal or urea denaturation. In RNase A, for example (Zhang et al., 1995), the extent of residual structure measured by hydrogen exchange methods is similar to that present in molten globules (Buck et al., 1994) and other well-characterized, partially structured proteins. The cold-denatured state of *Streptomyces* subtilisin inhibitor (Konno et al., 1995) shows a smaller radius of gyration by x-ray scattering than the heat- and urea-denatured states do—its value is only marginally (~5%) larger than that of the native state, and is in line with values cited for molten globules and other collapsed unfolded states. As a result, cold denaturation appears to be a milder method of denaturation than the more conventional

Received for publication 4 August 1997 and in final form 5 January 1998.

Address reprint requests to Dr. Jiri Jonas, Department of Chemistry, University of Illinois, 600 S. Mathews Ave., Urbana, IL 61801. Tel.: 217-333-2572; Fax: 217-244-3993; E-mail: J-Jonas@uiuc.edu.

© 1998 by the Biophysical Society

0006-3495/98/07/445/08 \$2.00

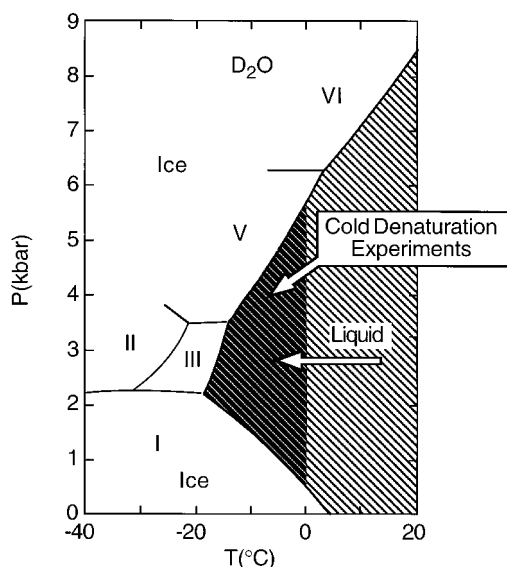


FIGURE 1 High-pressure phase diagram of D_2O (Jonas, 1982).

methods of heat and chemical (e.g., urea) denaturation. In contrast, the recent study of monomeric λ repressor (Huang and Oas, 1996) concludes that the heat- and cold-denatured states are thermodynamically and conformationally equivalent. However, this observation may be the result of the 3M urea added to the protein solutions used both for cold denaturation ($0^\circ C$) and heat denaturation ($70^\circ C$) of λ repressor.

Such results are interesting enough, but they become more important when related to modern protein folding studies. Structures that persist in a protein upon denaturation, even relatively mild denaturation, are likely to be highly stable. If no appreciable barriers exist to the rapid formation of such structures, they should be among the first to appear in the refolding of a protein. Consequently, mildly denatured states may serve as useful models for species present early in refolding, with the advantage that such species could be studied for hours or even days, rather than fractions of a second. There is already considerable evidence that the equilibrium collapsed unfolded states of some proteins, obtained under mildly denaturing conditions, are structurally similar to the early, collapsed states that occur when the protein begins to fold (Fink, 1995; Ptitsyn, 1995). Hence a major motivation for this research (Nash and Jonas, 1997a,b) was to characterize several proteins by cold denaturation and compare them to known species observed during folding.

The proteins discussed here were chosen for several reasons. All three—lysozyme, ribonuclease A, and ubiquitin—are small, well-characterized proteins that have been studied before. The solution NMR structures for all three are known (Di Stefano and Wand, 1987; Redfield and Dobson, 1988; Rico et al., 1991). Numerous studies have been made of all of these proteins in various denatured and partially folded states. For example, the folding pathways and inter-

mediates of ribonuclease A (Udgaonkar and Baldwin, 1990; Houry and Scheraga, 1996) and of lysozyme (Radford et al., 1992) have been described in detail. Various denatured states of ribonuclease A (Robertson and Baldwin, 1991), lysozyme (Buck et al., 1994), and ubiquitin (Harding et al., 1991) are available for comparison. The cold-denatured state of ribonuclease A has been characterized before (Zhang et al., 1995), and evidence for structure in the pressure-denatured state has been described. Furthermore, in the case of ubiquitin, Gladwin and Evans (1996) found no evidence for significant protection from exchange at early stages of folding; therefore, to test the hypothesis of this parallel, we have also investigated hydrogen exchange in the pressure-assisted, cold-denatured state of ubiquitin.

EXPERIMENTAL

The materials and experimental conditions for the various NMR experiments were discussed in detail in the original studies (Zhang et al., 1995; Nash et al., 1996; Nash and Jonas, 1997a,b). The principal NMR system in the laboratory is composed of a General Electric GN-300 NMR console, operating at a proton Larmor frequency of 300 MHz, with an Oxford Instruments wide-bore superconducting magnet ($\phi = 89$ mm, 7.04 T). The GN-300 is interfaced to a Tecmag Scorpio data acquisition system for pulse programming and experimental control with MacNMR software. This system was used for some studies of proteins at high pressure and ambient temperature (Ballard et al., 1996), as well as for optimization of cold denaturing conditions (i.e., determination of pressures and temperatures that lead to near-complete cold denaturation) for the hydrogen exchange experiments (Nash et al., 1996; Nash and Jonas, 1997a,b).

The hydraulic pressure generation system was similar to the system described previously (Jonas et al., 1993). As with the earlier system, carbon disulfide (CS_2) was used as the pressure transmitting fluid for proton studies. As an illustration of the quality of high-resolution NMR spectra during high-pressure denaturation experiments, we include Fig. 2 and Fig. 3, which are taken from our earlier studies.

For most of the recent protein studies, more advanced instrumentation (Ballard et al., 1998) was used. For general-purpose studies of proteins, the group has begun using a Varian INOVA wide-bore instrument, adapted to handle high pressure, with a proton frequency of 500 MHz. This instrument is gradually replacing the 300-MHz spectrometer for protein studies because of its higher sensitivity and resolution (Table 1), and is useful for direct measurements at high pressure at temperatures at and above room temperature (range $\sim 0^\circ C$ to $\sim 60^\circ C$).

For lower temperatures, other methods and instruments have been employed. Structure in cold-denatured proteins was assessed by hydrogen exchange techniques, which did not require high pressure to be maintained during measurement. Measurements of the extent of hydrogen exchange in cold-denatured proteins were therefore obtained on spectrometers outside the group laboratory: either a Varian Unity 500 MHz spectrometer (ribonuclease A) or a Varian INOVA 500 MHz narrow-bore spectrometer (lysozyme and ubiquitin), both using a conventional, commercially available NMR probe. Cold-denaturing conditions were obtained at pressures of 2250–3750 bar and temperatures of -13 to $-17^\circ C$, depending on the protein (Nash et al., 1996; Nash and Jonas, 1997a,b).

It is appropriate at this point to mention several design considerations for high-resolution, high-pressure NMR probes that are to be used for protein studies. The sample size (diameter) should definitely be greater than 5 mm; otherwise the sensitivity of the high-pressure NMR probe will seriously limit the scope of problems to be studied. For a protein it should be possible to obtain good S/N for concentrations in the millimolar (mM) or lower range. Higher concentrations usually result in aggregation and even precipitation of the protein when temperature or pressure is changed.

In our recent experiments (Ballard et al., 1998), we have increased the sensitivity, power, and tuning range of our double-tuned ($^1H/^2H$) NMR

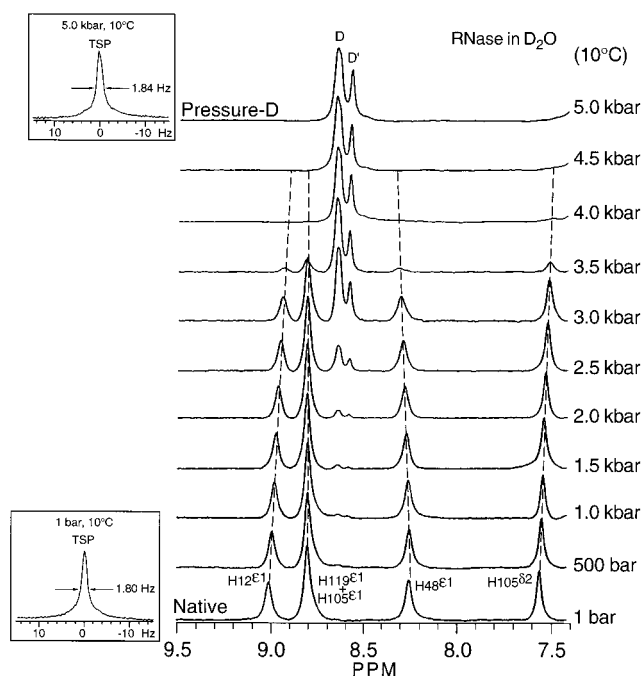


FIGURE 2 Histidine region of the ^1H NMR spectra of RNase A in D_2O at various pressures (10°C , $\text{pH}^* 2.0$). The standard in the insets is sodium 3-(trimethylsilyl)tetrauteriopropionate (TSP) (Zhang et al., 1995).

probes. The pressure vessel, pressure RF feedthroughs, and internal capacitor design concepts described earlier were all incorporated. In contrast, though, the RF coil now consists of a single-turn saddle coil machined from low magnetic susceptibility oxygen-free copper. Table 1 illustrates the significant improvement in sensitivity of the high-pressure NMR probe, when the coil design is changed from a two-turn wire coil to a one-turn machined coil by comparing the sensitivity (S/N ratio) for various high-pressure NMR probes used in our laboratory. For an 8-mm sample diameter, the S/N ratio for a 300-MHz probe increased from 34 to 131, whereas it increased to 260 at 500 MHz. Clearly, the increased frequency of 500 MHz also contributes to the enhanced sensitivity, but the major improvement is due to the RF coil design.

A comparison of the high quality of spectra obtained at 500 MHz with the new probe RF coil design to those obtained at 300 MHz with the earlier coil design is given in Fig. 4. The most important feature is the improved sensitivity, as the aromatic region, 500 MHz N-domain of troponin C F29W with Ca^{2+} was obtained for a 0.4 mM concentration compared to the 300 MHz spectrum, which was obtained for a 0.8 mM concentration of the protein using similar acquisition parameters. Although one can readily appreciate the advantages of higher sensitivity and probe power on dilute biochemical studies using one-pulse methods, we feel that an even more important extension of this work is in the field of high-pressure 2D NMR. As a demonstration of this capability, we include Fig. 5, which shows the 2D NOESY aromatic region of N-domain troponin C F29W at 5 kbar.

RESULTS AND DISCUSSION

The experimental procedures were described in detail in the original studies (Zhang et al., 1995; Nash et al., 1996; Nash and Jonas, 1997a,b) of cold denaturation of ribonuclease A, lysozyme, and ubiquitin. Hydrogen exchange data for proteins are typically expressed in terms of the protection factor $P = k_{\text{rc}}/k_{\text{obs}}$ for a given amide proton, where k_{obs} is the experimentally measured exchange rate and k_{rc} is the ex-

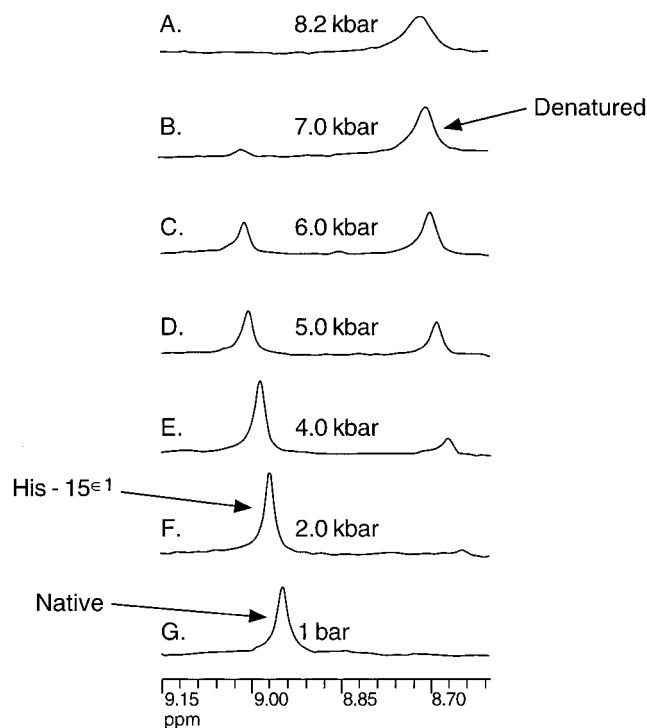


FIGURE 3 Stacked ^1H NMR plot of the lysozyme ($\text{pH}^* 2.2$, 4 mM protein, 20 mM maleic-2,3-*d*2 anhydride, 1.5 mM TSP) histidine region at selected pressures at 37.5°C . Note the disappearance of the native His^{15} residue peak (~ 8.95 ppm) and the appearance of the denatured His^{15} residue peak (~ 8.70 ppm) with pressure; complete denaturation is attained between 7 and 8.25 kbar (Ballard et al., 1996).

change rate for a proton in an ideal unstructured polypeptide under the same conditions. P values close to 1 indicate lack of appreciable structure, whereas P values in certain regions of native proteins can exceed 10^6 . In partially folded states, such as molten globules (Buck et al., 1994) or the methanol-induced A state of ubiquitin (Pan and Briggs, 1992), P values are intermediate. Typical values in such states range from 1 to several hundred.

The exchange of amide hydrogens in peptides is primarily caused by acid and base, with a small contribution from water, which can act as a weak acid or base (Bai et al., 1993):

$$k = k_a[\text{D}^+] + k_b[\text{OD}^-] + k_w \quad (1)$$

TABLE 1 High-pressure NMR probe performance features

Coil design	^1H freq. MHz [max. press., bars]	Sample		
		O.D. (mm)	S/N	Ref.
2-Turn wire coil,	300 [9000]	8	34	Ballard et al. (1996)
1-Turn machined coil, 300 MHz	300 [5000]	8	131	Ballard et al. (1998)
1-Turn machine coil, 500 MHz	500 [5000]	8	260	Ballard et al. (1998)

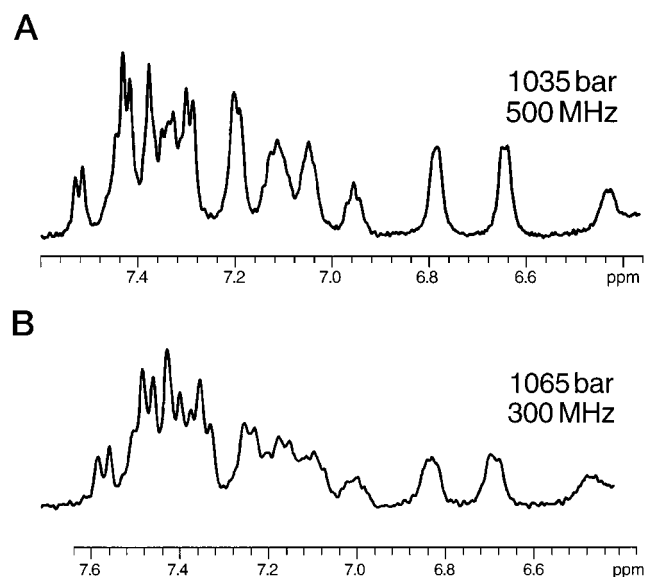


FIGURE 4 Comparison of the 1D proton aromatic region of the NMR spectrum of N-domain troponin C F29W + Ca^{2+} solution (pH* 7.0, 20 mM tris(hydroxymethyl)aminomethane-*d*11, 100 mM potassium chloride, 5 mM dithiothreitol, 2 mM ethylenebis(oxyethylenenitrilo)tetraacetic acid, 8 mM calcium chloride, 1.5 mM TSP) obtained at ~ 1 kbar pressure and 500 MHz (A) and 300 MHz (B). Spectrum A was obtained for a 0.4 mM protein solution, and spectrum B was recorded for a 0.8 mM protein solution. The number of accumulations was 1024 for both A and B.

Values for the three rate constants are known for reference “random coil” materials, specifically, unstructured oligopeptides and random-coil polypeptides, at 293 K and ambient pressure (Bai et al., 1993). To obtain a value for k_{rc} for cold-denaturing conditions, the reference values were corrected for temperature and pressure by using the activation energies and the activation volumes, respectively:

$$k_i(T) = k_i(T_0) \exp\left(-\frac{E_a}{R} \left[\frac{1}{T} - \frac{1}{T_0}\right]\right) \quad (2)$$

$$k_i(P) = k_i(P_0) \exp\left(-\frac{(P - P_0)\Delta V^\ddagger}{RT}\right) \quad (3)$$

where i denotes any of the three individual reactions and E_a and ΔV^\ddagger are the activation energy and activation volume. The activation volume, defined from

$$\Delta V^\ddagger = -RT \frac{\partial \ln k}{\partial P} \quad (4)$$

was assumed to be constant, over the pressure range of interest, to derive Eq. 3. This assumption has been shown to be valid over a wide pressure range for k_a and k_b in poly-D,L-lysine (Carter et al., 1978), and because the reaction mechanism for k_w is similar, this is a reasonable assumption here as well. The activation energies for k_a , k_b , and k_w are 14 kcal/mol, 3 kcal/mol, and 19 kcal/mol, respectively (Bai et al., 1993). Activation volumes were obtained from data on model compounds: random coil poly-D,L-lysine for k_a and k_b (Carter et al., 1978), and *N*-methylacetamide for k_w (Mabry

et al., 1996). The values of ΔV^\ddagger are 0 ± 1 , $+6 \pm 1$, and -9.0 ± 1.8 cm^3/mol for k_a , k_b , and k_w , respectively.

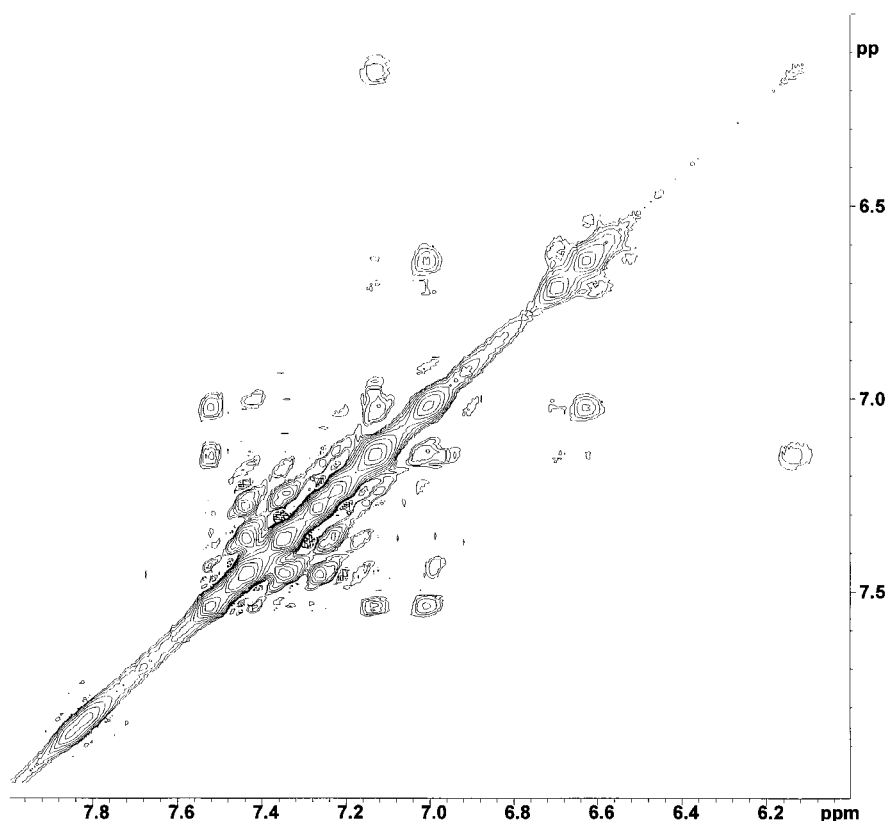
Fig. 6 A shows the protection factors in cold-denatured lysozyme ($T = -13^\circ\text{C}$, $p = 3750$ bar) as a function of residue number and their correspondence with secondary structural elements in the native state (Nash and Jonas, 1997a); Fig. 7 shows how the protection factors in cold-denatured lysozyme compare with those in various other well-studied denatured states—thermally denatured lysozyme at 69°C , chemically denatured lysozyme in 8 M urea solution, and the acid-denatured state of CM^{6-127} lysozyme, produced by cleaving the disulfide bond between C6 and C127 in native lysozyme (Buck et al., 1994).

From the hydrogen exchange rate data, it is clear that many regions of lysozyme are markedly protected from exchange, with P values exceeding 10, in the cold-denatured state. The range of P factors runs from 1.19 for F3 to 71.0 for R114. Except for a partially folded form observed in 50% trifluoroethanol (Buck et al., 1994), cold-denatured lysozyme is the only form of denatured lysozyme that shows appreciable protection from exchange. Data for heat, urea, and CM^{6-127} lysozyme, analyzed using the same temperature and side chain correction methods used in this study (Buck et al., 1994), show few residues with $P > 5$ (Fig. 6). It should be made clear that the pressure-assisted, cold-denatured state is not a “pure” cold-denatured state, because the pressure affects the protein directly. Nevertheless, any effect that pressure has is clearly very different from that induced by high temperature or chemical denaturants such as urea.

Lysozyme, in its native state, consists of two domains: the α domain, which contains four α -helices, and the β -domain, which contains a three-strand antiparallel β -sheet (Miranker et al., 1991). In the cold-denatured state of lysozyme, protection of amide protons against exchange is largely confined to the α -domain; all four α -helices show appreciable protection ($P > 10$ for at least one residue) from exchange. The most notable protection, involving three residues with $P > 30$, occurs in helix D (residues 108–115). In contrast, most of the β -sheet region (residues 41–60) shows no appreciable protection, with all but two residues having $P < 5$. The persistence of α -helical structure in cold-denatured proteins has been noted before, as in the cold-denatured state of barstar (Wong et al., 1996). An anomalous area of protection occurs at the end of the β -sheet and in the following loop, a region in which residues 60, 61, 63, 64, 65, 76, and 78 were observable. This region is the most highly protected area of cold-denatured lysozyme, after the D helix. It differs from the other highly protected regions in cold-denatured lysozyme, though, by not consisting of a single, well-defined region of secondary structure.

By using pulsed-labeling hydrogen exchange studies and confining exchange to the dead time of their instrumentation (~ 3.5 ms), Gladwin and Evans (1996) observed relatively early stages in the folding of lysozyme. Slowing of exchange measured during this time can be quantified by

FIGURE 5 2D $^1\text{H}/^1\text{H}$ NOESY aromatic region of N-domain troponin C F29W + Ca^{2+} obtained with the 500-MHz probe (25°C) at 5 kbar. The protein concentration was ~ 0.6 mM, and the NOESY mixing time was 0.15 s. The composition of the buffer solution was identical to that used in Fig. 4.



comparing the measured exchange rate to that for a random coil, as in other hydrogen exchange studies. The resulting quantity, although similar to a protection factor, is determined from a rate that changes considerably as the protein refolds; as a result, it is best referred to as a “dead-time inhibition factor” (I_D) rather than a true protection factor (Gladwin and Evans, 1996). Nevertheless, I_D values provide information similar to that provided by P values in equilibrium denatured states. During the first 3.5 ms of folding, lysozyme shows moderate degrees of protection ($I_D > 5$), not only in the α -helices and the C-terminal 3^{10} helix, but also in the loop region from residues 60–65, as well as residue 78 (Gladwin and Evans, 1996). We have thus observed a strong parallel between a stable, denatured form of lysozyme and the transient species observed during folding. Fig. 6 B compares the inhibition of hydrogen exchange observed during the first 3.5 ms of folding (Gladwin and Evans, 1996) to the protection factors obtained for pressure-assisted, cold-denatured lysozyme, as shown in Fig. 6 A.

The range of protection factors observed (Nash et al., 1996) in cold-denatured RNase A (2.8–78) is similar to that present in cold-denatured lysozyme. In contrast to lysozyme, however, the extent of protection in cold-denatured RNase A is less organized. Rather than having large extents of secondary structure protected, such as large portions of the α -helices in lysozyme, the protection in cold-denatured RNase A occurs in small regions, particularly those near disulfide-linked cysteine residues. Fig. 8 plots the protection factors versus residue in pressure-assisted cold-denatured

RNase A on a three-dimensional representation of the native structure. The most notable such region of high protection in RNase A, three residues with $P > 10$, is centered in C84, in the central strand of the large β -sheet. Protection in this β -sheet is highly nonuniform. For example, the region of the first strand from residues 35 to 48 is essentially unprotected ($P < 5$ for all residues), in contrast to the region around C84.

In a qualitative comparison, one can see that the pressure-assisted cold-denatured state exhibits patterns of protection factors (relatively low) resembling the pattern of protection factors observed by Udgaonkar and Baldwin (1990) and Houry and Scheraga (1996) for the folding intermediate of ribonuclease A. Fig. 8 also gives a qualitative comparison of protection factors for the early folding intermediate (Udgaonkar and Baldwin, 1990) and those observed of hydrogen exchange in the pressure-assisted cold-denatured state of ribonuclease A.

In the case of lysozyme and RNase A, the patterns of protection against hydrogen exchange are similar to those observed in early (refolding time < 10 ms) folding intermediates for these proteins, leading to the idea that the cold-denatured state is structurally similar to such intermediates. To help test this idea, ubiquitin, which has folding kinetics that are markedly different from those of either RNase A or lysozyme (Briggs and Roder, 1992), was investigated (Nash and Jonas, 1997b). In particular, ubiquitin shows much less evidence of early structure formation than lysozyme; it more closely resembles a random coil.

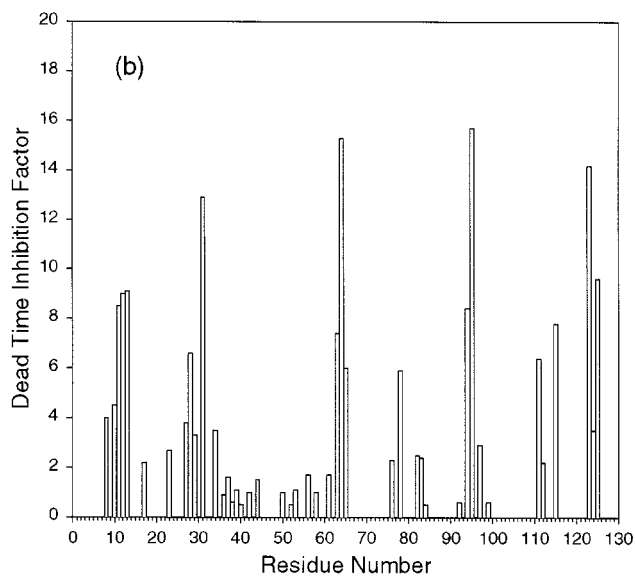
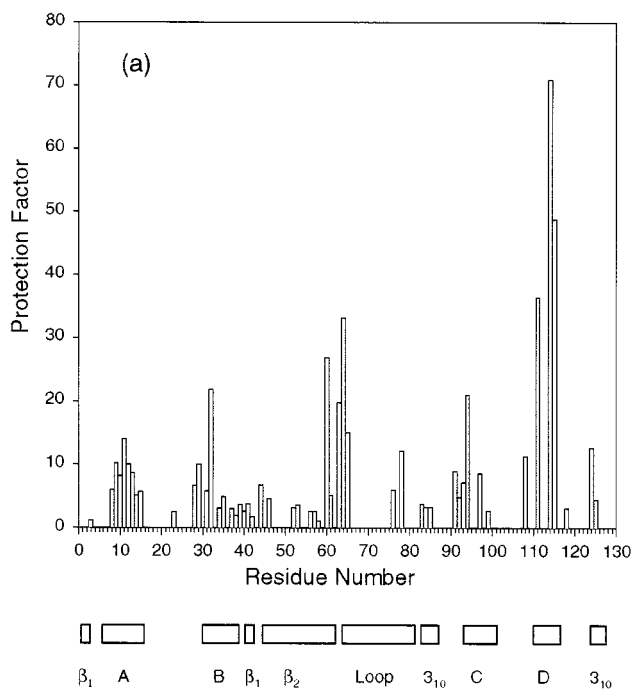


FIGURE 6 (a) Protection factors for the pressure-assisted cold-denatured state ($p = 3750$ bar, $T = -13^\circ\text{C}$) of lysozyme. Secondary structural elements in the native state are indicated below. A–D denote the four α -helices; β_1 and β_2 denote the two- and three-stranded β -sheet regions, respectively. (b) Dead-time inhibition factors obtained for the first 3.5 ms of lysozyme folding (Gladwin and Evans, 1996).

Cold-denatured ubiquitin ($p = 2250$ bar, $T = -16^\circ\text{C}$) shows little deviation from a random coil in its hydrogen exchange kinetics, with no P values above 5 and most below 2. As shown in Fig. 8, these values are typical of highly denatured proteins such as the urea-denatured state of lysozyme. Under other circumstances, however, such as the A state produced by a 60% methanol solution at a pH of 2.0, ubiquitin shows significantly more protection from ex-

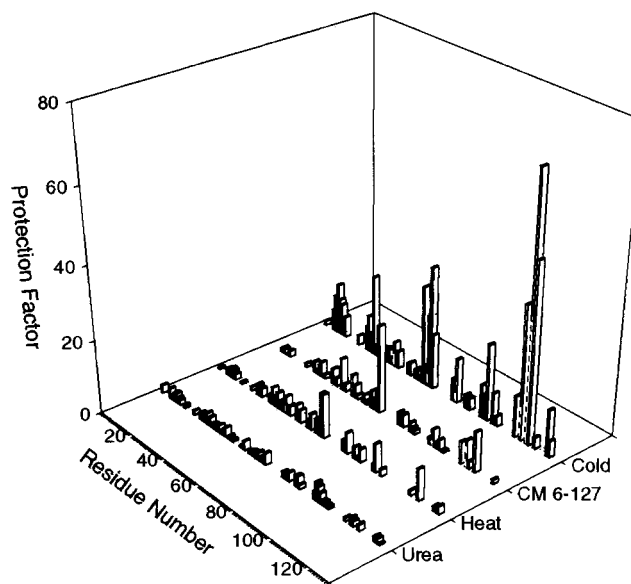


FIGURE 7 Comparison of protection factors observed in various experiments. Data for cold-denatured lysozyme were taken from Nash and Jonas (1997a); data for heat, urea, and acid-denatured CM⁶⁻¹²⁷ lysozyme were taken from Buck et al. (1994).

change. It is important to point out that in ubiquitin, the same dead-time inhibition study (Gladwin and Evans, 1996) showed no evidence for protection from exchange, with the largest dead-time inhibition factors being ~ 2 (Fig. 9). Moreover, there was no correlation of even these modestly

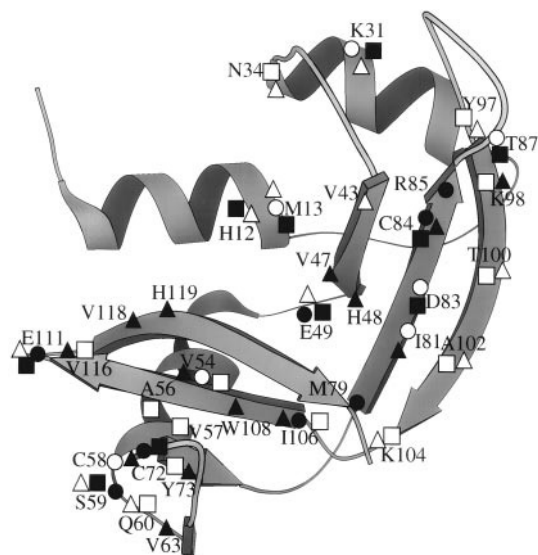


FIGURE 8 Qualitative comparison of protection factors for the pressure-denatured state (Zhang et al., 1995) and pressure-assisted cold-denatured state (Nash and Jonas, 1996) of RNase A compared to protection factors for early folding intermediate for RNase (Udgaonkar and Baldwin, 1990). Amide protons are protected in pressure-denatured state with $p > 10$, < 20 (\circ); pressure-denatured state with $p > 20$ (\bullet); cold-denatured state with $p > 10$, < 20 (\square); cold-denatured state with $p > 20$ (\blacksquare); folding intermediate with "strong" protection (\triangle); and folding intermediate with "weak," "medium," or "ill-defined" protection (\blacktriangle).

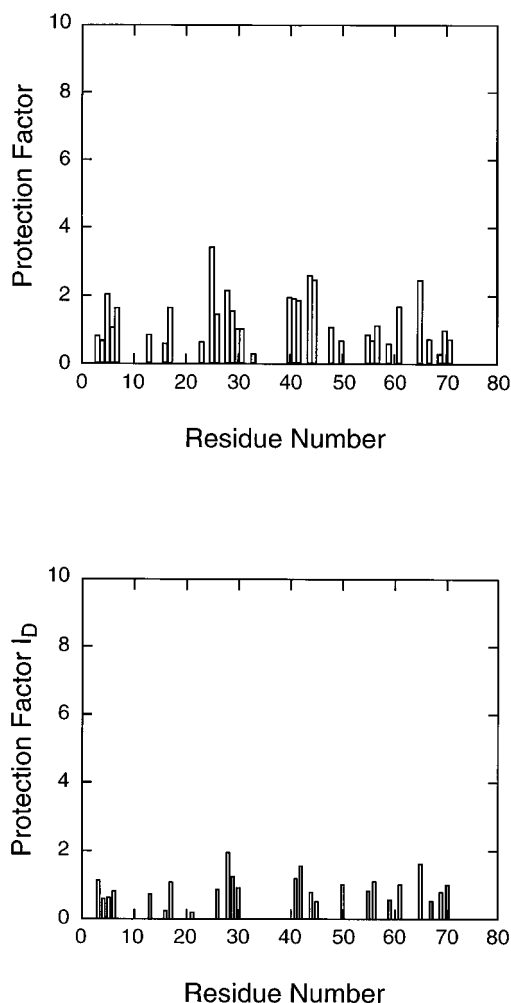


FIGURE 9 Protection factors versus residue in pressure-assisted cold-denatured ($T = -16^{\circ}\text{C}$, $p = 2250$ bar) ubiquitin (A) compared with dead-time exchange inhibition factors (B) (protection factor I_D obtained during the first 3.5 ms of refolding; Gladwin and Evans, 1996).

elevated factors within significant elements of secondary structure, as there were in lysozyme.

The similarity of cold-denatured state protection factors to the protection observed in protein refolding studies has led to the idea that the cold-denatured state is populated by species comprising elements of secondary and perhaps tertiary structure that are comparatively stable. The similarities between the cold-denatured state and the early folding states suggest that these structural elements would be expected to form first during folding. In the case of ubiquitin, the folding reaction appears to proceed in one highly cooperative step, with little of the multiphasic behavior observed in proteins like lysozyme or ribonuclease A. Although a possible intermediate for ubiquitin refolding has been characterized by other means (Khorasanizadeh et al., 1996), the intermediate thus identified shows no protection from hydrogen exchange. The results for the cold-denatured state of ubiquitin parallel these results: there is no partially folded state that is stable enough to be characterized by hydrogen exchange methods when ubiquitin is cold denatured.

Work is in progress in our laboratory to investigate systematically the pressure- and pressure-assisted cold denaturation of other proteins, to obtain novel information about their folding intermediates, or to simply indicate key stable structures favored preferentially in the folding process. The methods used to investigate these states include both the hydrogen exchange method outlined above and more direct NMR methods (e.g., COSY, NOESY, and TOCSY) using the improved high-pressure NMR probes (Table 1) and the 500-MHz NMR instrument.

Our thanks are due to Ms. Jo Anna Gates for providing Fig. 8.

This work was supported in part by the National Institutes of Health (National Institutes of Health) under grant PHS 5 RO1 GM42452-09 and the National Science Foundation under grant NSF CHE 95-26237. Some of the NMR data used for this work were collected on a spectrometer at the University of Illinois School of Chemical Sciences Varian/Oxford Instrument Center for Excellence in NMR Laboratory. We acknowledge National Institutes of Health grant 1-S10-RR-10444-01, the Keck Foundation, and the Beckman Institute for their contributions to this laboratory.

REFERENCES

- Anfinsen, C. B. 1973. Principles that govern the folding of protein chains. *Science*. 181:223–230.
- Bai, Y., J. S. Milne, L. Mayne, and S. W. Englander. 1993. Primary structure effects on peptide group hydrogen exchange. *Proteins Struct. Funct. Genet.* 17:75–86.
- Ballard, L., C. Reiner, and J. Jonas. 1996. High-resolution NMR probe for experiments at high pressures. *J. Magn. Res.* 123A:81–86.
- Ballard, L., A. Yu, C. Reiner, and J. Jonas. 1998. A high pressure, high resolution NMR probe for experiments at 500 MHz. *J. Magn. Res.* (in press).
- Briggs, M. S., and H. Roder. 1992. Early hydrogen-bonding events in the folding reaction of ubiquitin. *Proc. Natl. Acad. Sci. USA*. 89:2017–2021.
- Buck, M., S. E. Radford, and C. M. Dobson. 1994. Amide hydrogen exchange in a highly denatured state: hen egg-white lysozyme in urea. *J. Mol. Biol.* 237:247–254.
- Carter, J. V., D. G. Knox, and A. Rosenberg. 1978. Pressure effects on folded proteins in solution. *J. Biol. Chem.* 253:1947–1953.
- Creighton, T. E. 1993. *Proteins*, 2nd ed. W. H. Freeman and Company, New York.
- Di Stefano, D. L., and A. J. Wand. 1987. Two-dimensional ^1H NMR study of human ubiquitin: a main chain directed assignment and structure analysis. *Biochemistry*. 26:7272–7281.
- Fink, A. L. 1995. Compact intermediate states in protein folding. *Annu. Rev. Biophys. Biomol. Struct.* 24:495–522.
- Gladwin, S. T., and P. A. Evans. 1996. Structure of very early protein folding intermediates: new insights through a variant of hydrogen exchange labeling. *Folding Des.* 1:407–417.
- Harding, M. H., D. H. Williams, and D. N. Woolfson. 1991. Characterization of a partially denatured state of a protein by two-dimensional NMR: reduction of the hydrophobic interactions in ubiquitin. *Biochemistry*. 30:3120–3128.
- Houry, W. A., and H. A. Scheraga. 1996. Structure of a hydrophobically collapsed intermediate on the conformational folding pathway of ribonuclease A probed by hydrogen-deuterium exchange. *Biochemistry*. 35:11734–11746.
- Huang, G. S., and T. G. Oas. 1996. Heat and cold denatured states of monomeric λ repressor are thermodynamically and conformationally equivalent. *Biochemistry*. 35:6173–6180.
- Jonas, J. 1982. Nuclear magnetic resonance at high pressure. *Science*. 216:1179–1184.
- Jonas, J., and A. Jonas. 1994. High-pressure NMR spectroscopy of proteins and membranes. *Annu. Rev. Biophys. Biomol. Struct.* 23:287–318.

- Jonas, J., X. Peng, P. Koziol, C. Reiner, and D. M. Campbell. 1993. High-resolution NMR spectroscopy at high pressures. *J. Magn. Reson.* 102B:299–309.
- Khorasanizadeh, S., I. D. Peters, and H. Roder. 1996. Evidence for a three-state model of protein folding from kinetic analysis of ubiquitin variants with altered core residues. *Nature Struct. Biol.* 3:193–205.
- Kim, P. S., and R. L. Baldwin. 1990. Intermediates in the folding reactions of small proteins. *Annu. Rev. Biochem.* 59:631–660.
- Konno, T., M. Kataoka, Y. Kamatari, K. Kanaori, A. Nosaka, and K. Akasaka. 1995. Solution x-ray scattering analysis of cold-, heat-, and urea-denatured states in a protein, *Streptomyces subtilisin inhibitor*. *J. Mol. Biol.* 251:95–103.
- Mabry, S. A., B.-S. Lee, T. Zheng, and J. Jonas. 1996. Determination of the activation volume of the uncatalyzed hydrogen exchange reaction between *n*-methylacetamide and water. *J. Am. Chem. Soc.* 118:8887–8890.
- Miranker, A., S. E. Radford, M. Karplus, and C. M. Dobson. 1991. Demonstration by NMR of folding domains in lysozyme. *Nature*. 349:633–636.
- Nash, D., and J. Jonas. 1997a. Structure of pressure-assisted cold denatured lysozyme and comparison with lysozyme folding intermediates. *Biochemistry*. 36:14375–14383.
- Nash, D., and J. Jonas. 1997b. Structure of the pressure-assisted cold denatured state of ubiquitin. *Biochem. Biophys. Res. Commun.* 238:289–291.
- Nash, D., B.-S. Lee, and J. Jonas. 1996. Hydrogen-exchange kinetics in the cold denatured state of ribonuclease A. *Biochim. Biophys. Acta.* 1297:40–48.
- Pan, Y., and M. S. Briggs. 1992. Hydrogen exchange in native and alcohol forms of ubiquitin. *Biochemistry*. 31:11405–11412.
- Ptitsyn, O. B. 1995. Structures of folding intermediates. *Curr. Opin. Struct. Biol.* 5:74–78.
- Radford, S. E., C. M. Dobson, and P. A. Evans. 1992. The folding of hen lysozyme involves partially structured intermediates and multiple pathways. *Nature*. 358:302–307.
- Redfield, C., and C. M. Dobson. 1988. Sequential ¹H NMR assignments and secondary structure of hen egg white lysozyme in solution. *Biochemistry*. 27:122–136.
- Rico, M., J. Santoro, C. González, M. Bruix, J. L. Neira, J. L. Nieto, and J. Herranz. 1991. 3D structure of bovine pancreatic ribonuclease A in aqueous solution: an approach to tertiary structure determination from a small basis of ¹H NMR NOE correlations. *J. Biomol. NMR.* 1:283–298.
- Robertson, A. D., and R. L. Baldwin. 1991. Hydrogen exchange in thermally denatured ribonuclease A. *Biochemistry*. 30:9907–9914.
- Udgaonkar, J. B., and R. L. Baldwin. 1990. Early folding intermediate of ribonuclease A. *Proc. Natl. Acad. Sci. USA.* 87:8197–8201.
- Weber, G., and H. G. Drickamer. 1983. The effect of high pressure upon proteins and other biomolecules. *Q. Rev. Biophys.* 16:89–112.
- Wong, K.-B., S. M. V. Freund, and A. R. Fersht. 1996. Cold denaturation of barstar: ¹H, ¹⁵N, and ¹³C NMR assignment and characterisation of residual structure. *J. Mol. Biol.* 259:805–818.
- Zhang, J., X. Peng, A. Jonas, and J. Jonas. 1995. NMR study of the cold, heat, and pressure unfolding of ribonuclease A. *Biochemistry*. 34:8631–8641.